

Synthesis, Characterization, and Crystal Structure of $[\text{PPN}][\text{Re}_7\text{C}(\text{CO})_{21}(\text{P}(\text{O}^-\text{Ph})_3)]$. Illustration of a Polar Intermediate Stage in Cluster Decapping

Scott W. Simerly, Scott R. Wilson, and John R. Shapley*

School of Chemical Sciences and the Materials Research Laboratory, University of Illinois, Urbana, Illinois 61801

Received August 13, 1991

Introduction

Oxidatively induced substitution of anionic metal carbonyl clusters,¹ in effect the replacement of two negative charges by a two-electron donor, is an increasingly important tool in the synthesis of substituted cluster compounds. This approach has been employed with particular success in the formation of derivatives of $[\text{Ru}_6\text{C}(\text{CO})_{16}]^{2-}$,²⁻⁴ and other notable developments include, as examples, the oxidation of $[\text{Os}_7(\text{CO})_{20}]^{2-}$ in the presence of carbon monoxide to form $[\text{Os}_7(\text{CO})_{21}]^{2-}$,⁴ the analogous transformation of $[\text{Re}_7\text{C}(\text{CO})_{21}]^{3-}$ into $[\text{Re}_7\text{C}(\text{CO})_{22}]^{-}$,⁵ and the formation of $[\text{Ir}_6(\text{CO})_{14}(\text{C}_2\text{Ph}_2)]$ from $[\text{Ir}_6(\text{CO})_{15}]^{2-}$.⁶

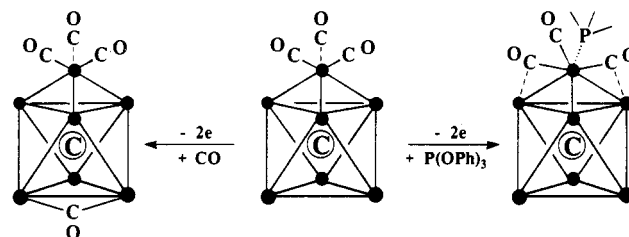
On the other hand, oxidation can lead to unpredictable changes in nuclearity, as in the oxidation of $[\text{Ir}_6(\text{CO})_{15}]^{2-}$ with Cu^+ to give $[\text{Ir}_{12}(\text{CO})_{26}]^{2-}$ ⁷ or the formation of $[\text{Re}_6\text{C}(\text{CO})_{19}]^{2-}$ from treatment of $[\text{Re}_7\text{C}(\text{CO})_{21}]^{3-}$ with iodine.⁸ We have recently shown that ferrocenium oxidation of $[\text{Re}_7\text{C}(\text{CO})_{21}]^{3-}$ in the presence of PPh_3 also forms $[\text{Re}_6\text{C}(\text{CO})_{19}]^{2-}$,⁹ but no intermediate substitution product could be characterized. We have now found that two-electron oxidation of $[\text{Re}_7\text{C}(\text{CO})_{21}]^{3-}$ in the presence of $\text{P}(\text{O}^-\text{Ph})_3$ leads to $[\text{Re}_7\text{C}(\text{CO})_{21}(\text{P}(\text{O}^-\text{Ph})_3)]^{-}$, which can be isolated and fully characterized. The unique structure of this species, defined both by X-ray crystallography and by variable-temperature ¹³C NMR spectra, serves to illustrate an intermediate stage in the loss of a metal vertex to form $[\text{Re}_6\text{C}(\text{CO})_{19}]^{2-}$. Furthermore, the structure of $[\text{Re}_7\text{C}(\text{CO})_{21}(\text{P}(\text{O}^-\text{Ph})_3)]^{-}$ forms a contrast with that of isoelectronic $[\text{Re}_7\text{C}(\text{CO})_{22}]^{-}$ (Scheme I).

Experimental Section

General Procedures. All reactions were carried out under a nitrogen atmosphere with the use of standard Schlenk techniques. Solvents were stored over drying agents and distilled under nitrogen prior to use. $[\text{PPN}]_3[\text{Re}_7\text{C}(\text{CO})_{21}]^{10}$ and $[\text{Cp}_2\text{Fe}][\text{PF}_6]$ ¹¹ were prepared by literature methods, and their combination in the presence of CO produced $[\text{PPN}][\text{Re}_7\text{C}(\text{CO})_{22}]$.⁹ $\text{P}(\text{O}^-\text{Ph})_3$ (Aldrich) and $[\text{PPN}][\text{Cl}]$ (Aldrich) were used as received.

Infrared spectra were recorded on a Perkin-Elmer Model 1750 FT-IR spectrometer. ³¹P NMR spectra were recorded at 121 MHz with a General Electric GN-300 spectrometer and are referenced to external H_3PO_4 . ¹³C VT-NMR spectra were recorded on a General Electric GN-500 spectrometer at 125 MHz for $[\text{PPN}][\text{Re}_7\text{C}(\text{CO})_{22}]$ and on a Nicolet NT-360 spectrometer at 90 MHz for $[\text{PPN}][\text{Re}_7\text{C}(\text{CO})_{21}(\text{P}(\text{O}^-\text{Ph})_3)]$. Samples for ¹³C NMR studies were synthesized from ca. 50% ¹³C-

Scheme I



enriched $[\text{PPN}]_3[\text{Re}_7\text{C}(\text{CO})_{21}]$.¹¹ Fast atom bombardment (FAB) mass spectra were obtained with a matrix of dithioerythritol/dithiothreitol and xenon atom bombardment spectra on a ZAB-SE mass spectrometer by the staff of the Mass Spectrometry Center of the School of Chemical Sciences. Elemental analyses were performed by the Microanalytical Laboratory of the School of Chemical Sciences.

$[\text{PPN}][\text{Re}_7\text{C}(\text{CO})_{21}(\text{P}(\text{O}^-\text{Ph})_3)]$. $[\text{Cp}_2\text{Fe}][\text{PF}_6]$ (11.7 mg, 0.035 mmol) was added to a stirred dichloromethane solution of $[\text{PPN}]_3[\text{Re}_7\text{C}(\text{CO})_{21}]$ (52.3 mg, 0.015 mmol) and $\text{P}(\text{O}^-\text{Ph})_3$ (0.2 mL, 0.76 mmol). The color of the solution changed from red to dark green. After 20 min, the solvent was removed under vacuum, and the oily green residue was washed with hexane (10 mL) and then extracted into diethyl ether (50 mL). The ether solution was concentrated to a small volume (ca. 2 mL), and then hexane (ca. 10 mL) was layered on top. After solvent diffusion for 2 days at -20°C , dark green crystals were collected and dried (31.6 mg, 0.011 mmol, 77%). Anal. Calcd for $\text{C}_{76}\text{H}_{45}\text{NO}_{24}\text{P}_3\text{Re}_7$: C, 33.16; H, 1.65; N, 0.51; P, 3.38. Found: C, 33.27; H, 1.59; N, 0.56; P, 3.26. IR ($\text{CH}_2\text{-Cl}_2$): $\nu(\text{CO})$, 2067 (w), 2011 (vs), 1984 (w), 1942 (w) cm^{-1} . ¹³C NMR (20°C , CH_2Cl_2): δ 420.4 ($\mu\text{-C}$), 192.7 (Re-CO). ³¹P NMR (20°C , CH_2Cl_2): 100.9 ppm. FAB-MS (negative ion): m/z (¹⁸⁷Re) 2215 (M - PPN), 2186 (M - PPN - CO), 2094 (M - PPN - CO - OPh), 1905 ($\text{Re}_7\text{C}(\text{CO})_{21}$).

Conversion of $[\text{PPN}][\text{Re}_7\text{C}(\text{CO})_{21}(\text{P}(\text{O}^-\text{Ph})_3)]$ to $[\text{PPN}]_2[\text{Re}_6\text{C}(\text{CO})_{19}]$. $\text{P}(\text{O}^-\text{Ph})_3$ (0.1 mL, 0.38 mmol) was added to a stirred acetonitrile solution of $[\text{PPN}][\text{Re}_7\text{C}(\text{CO})_{21}(\text{P}(\text{O}^-\text{Ph})_3)]$ (49.4 mg, 0.018 mmol). After 30 min, the green solution had become red. The strong IR band of $[\text{Re}_7\text{C}(\text{CO})_{21}(\text{P}(\text{O}^-\text{Ph})_3)]^{-}$ at 2011 cm^{-1} had disappeared, and strong bands at 1994 and 1979 cm^{-1} due to $[\text{Re}_6\text{C}(\text{CO})_{19}]^{2-}$ had appeared. $[\text{PPN}][\text{Cl}]$ (15 mg, 0.026 mmol) was added, and the solvent was removed under vacuum. The red residue was dissolved in a minimum of dichloromethane, and 2-propanol was layered carefully on top. Solvent diffusion for 2 days at room temperature resulted in red crystals of $[\text{PPN}]_2[\text{Re}_6\text{C}(\text{CO})_{19}]$ (20.2 mg, 0.007 mmol, 41%), identified by its IR spectrum.⁶

In a separate experiment conducted under a CO atmosphere, a sample of the reaction mixture was evaporated, and a positive-ion FAB mass spectrum of the residue was obtained. The spectrum showed ion multiplets at m/z 932, 891, and 863, identified as $[\text{Re}(\text{CO})_3(\text{P}(\text{O}^-\text{Ph})_3)_2(\text{NCCH}_3)]^+$, $[\text{Re}(\text{CO})_3(\text{P}(\text{O}^-\text{Ph})_3)_2]^+$, and $[\text{Re}(\text{CO})_2(\text{P}(\text{O}^-\text{Ph})_3)_2]^+$, respectively.

X-ray Structural Determination. Table I provides a summary of the structural determination of $[\text{PPN}][\text{Re}_7\text{C}(\text{CO})_{21}(\text{P}(\text{O}^-\text{Ph})_3)]$. Dark green crystals were grown by solvent diffusion from a dichloromethane/methanol solution at room temperature. The selected crystal was cut from an acicular parent that had well-developed faces, and it was mounted on a glass fiber with epoxy. Diffraction data were collected at 27°C on a Syntex P2₁ four-circle diffractometer equipped with Crystal Logic automation. Lorentz, polarization, anomalous dispersion, extinction, and absorption corrections were applied to the data.

The structure was solved by direct methods (SHELXS-86). Correct positions for the metal atoms were deduced from an *E* map. Subsequent least-squares refinement and difference Fourier calculations revealed positions for the remaining non-hydrogen atoms. Phenyl rings were refined as ideal rigid groups, and hydrogen atoms were included as fixed contributors in idealized positions. Disordered carbonyl groups, C52-O52 A (relative site occupancy 0.67 (2)) and B were constrained to equivalent bond lengths. Common isotropic thermal parameters were varied for hydrogen atoms and the disordered carbonyl atoms, independent isotropic thermal coefficients were refined for phenyl carbon atoms, and the remaining atoms were refined with anisotropic thermal coefficients. The highest peaks in the final difference Fourier map were in the vicinity of the metal atoms. Fractional coordinates for the cluster anion are given in Table II, and selected bond lengths and angles are provided in Table III. Complete lists of coordinates, bond lengths, and bond angles are available as supplementary material.

- (1) Drake, S. R. *Polyhedron* 1990, 9, 455.
- (2) Ansell, G. B.; Bradley, J. S. *Acta Crystallogr., Sect. B* 1980, 36, 1939.
- (3) Drake, S. R.; Johnson, B. F. G.; Lewis, J. J. *Chem. Soc., Dalton Trans.* 1989, 243.
- (4) (a) Drake, S. R.; Johnson, B. F. G.; Lewis, J.; Conole, G.; McPartlin, M. J. *Chem. Soc., Dalton Trans.* 1990, 995. (b) Drake, S. R.; Johnson, B. F. G.; Lewis, J. J. *Chem. Soc., Chem. Commun.* 1988, 1033.
- (5) Beringhelli, T.; D'Alfonso, G.; De Angelis, M.; Ciani, G.; Sironi, A. J. *Organomet. Chem.* 1987, 322, C21.
- (6) Ceriotti, A.; Della Pergola, R.; Demartin, F.; Garlaschelli, L.; Manassero, M.; Masciocchi, N. *Organometallics* 1992, 11, 756.
- (7) Della Pergola, R.; Demartin, F.; Garlaschelli, L.; Manassero, M.; Martinengo, S.; Sansoni, M. *Inorg. Chem.* 1987, 26, 3487.
- (8) Beringhelli, T.; D'Alfonso, G.; Molinari, H.; Sironi, A. J. *Chem. Soc., Dalton Trans.* 1992, 689.
- (9) Hsu, G.; Wilson, S. R.; Shapley, J. R. *Inorg. Chem.* 1991, 30, 3882.
- (10) Hayward, C.-M. T.; Shapley, J. R. *Organometallics* 1988, 7, 448.
- (11) Hendrickson, D. N.; Sohn, Y. S.; Gray, H. B. *Inorg. Chem.* 1971, 10, 1559.

Table I. Crystallographic Data for [PPN][Re₇C(CO)₂₁(P(OPh)₃)]

formula	C ₇₆ H ₄₅ NO ₂₄ P ₃ Re ₇	fw	2752.5
temp	27 °C	λ	0.710 73 Å (Mo Kα)
size	0.2 × 0.2 × 0.2 mm	ρ _{calcd}	2.342 g cm ⁻³
space grp	P1, triclinic	μ	110.94 cm ⁻¹
a	13.214 (1) Å	transm coeff	0.220–0.112
b	13.946 (1) Å	2θ max (octs)	45° (±h, ±k, ±l)
c	21.493 (2) Å	I _{tot} (unique, R _i)	11 068 (10 194, 0.034)
α	89.427 (6)°	I > 2.58σ(I)	5788
β	81.615 (6)°	final ΔF map	–0.94 to +1.02 e/Å ³
γ	85.028 (6)°	R ^a	0.039
V	3903 (1) Å ³	R _w ^b	0.048
Z	2		

^a $R = \sum ||F_o| - |F_c|| / \sum |F_o|$, ^b $R_w = [\sum w(|F_o| - |F_c|)^2 / \sum w|F_o|^2]^{1/2}$; $w = k / [(σ(F_o))^2 + (pF_o)^2]$, $k = 1.98$, $p = 0.017$.

Results

Oxidation of [PPN]₃[Re₇C(CO)₂₁] with 2 equiv of [Cp₂Fe]-[PF₆] in the presence of excess P(OPh)₃ rapidly forms [PPN]-[Re₇C(CO)₂₁(P(OPh)₃)], which has been isolated as air-stable green crystals in 77% yield and characterized by analytical and spectroscopic data as well as by X-ray crystallography. A diagram of the molecular structure is shown in Figure 1, and Table III lists selected bond lengths and angles. Variable-temperature ¹³C NMR spectra of [PPN][Re₇C(CO)₂₁(P(OPh)₃)] and of [PPN]-[Re₇C(CO)₂₂] are shown in Figures 2 and 3, respectively. In acetonitrile with excess P(OPh)₃, [Re₇C(CO)₂₁(P(OPh)₃)]⁻ is quickly converted to [Re₆C(CO)₁₉]²⁻.

Discussion

Structural Features of [Re₇C(CO)₂₁(P(OPh)₃)]⁻. The solid-state structure of [PPN][Re₇C(CO)₂₁(P(OPh)₃)] is a monocapped octahedron (see Figure 1), as seen previously for [NEt₄][Re₇C(CO)₂₂]⁵ and [NEt₄]₃[Re₇C(CO)₂₁].¹² The Re₇ framework is as expected from other Re₇^{12–14} and Re₇M^{15–19} structures, with the average Re–Re bond length within 0.01 Å of that observed for [Re₇C(CO)₂₂]⁻.⁵ The striking feature of the structure of [Re₇C(CO)₂₁(P(OPh)₃)]⁻ in comparison with that of [Re₇C(CO)₂₂]⁻ is the position of the “extra”, i.e., 22nd, ligand. For both compounds, the rhenium atoms forming the Re₆C octahedral core are each bonded to three terminal carbonyls. For [Re₇C(CO)₂₂]⁻, the capping rhenium atom also has three carbonyls, and the extra carbonyl bridges an edge of the triangular face opposite the cap. For [Re₇C(CO)₂₁(P(OPh)₃)]⁻, the capping rhenium center (Re7) is coordinated to four ligands—the phosphite as well as three carbonyls. Two of these carbonyl ligands (CO71, CO73), with a respective pseudo-trans orientation, are slightly bent (average ∠(Re–C–O) = 165 (2)°) due to semibridging interactions with two rhenium atoms of the capped face (Re2...C71, Re3...C73, average *d*(Re...C) = 3.02 (10) Å, average ∠(Re...C–O) = 124 (2)°). The phosphite ligand is oriented over the third rhenium atom (Re1) in this face, so that the remaining carbonyl ligand (CO72) is positioned over the midpoint of the opposite Re2–Re3 bond.

The bonding interactions of a ML₄ fragment capping a triangular face, such as Os(CO)₄ interacting with Os₃(CO)₉²⁻, have been discussed.²⁰ A C_{2v} geometry is favored for the ML₄

Table II. Important Positional Parameters^a for [PPN][Re₇C(CO)₂₁(P(OPh)₃)]

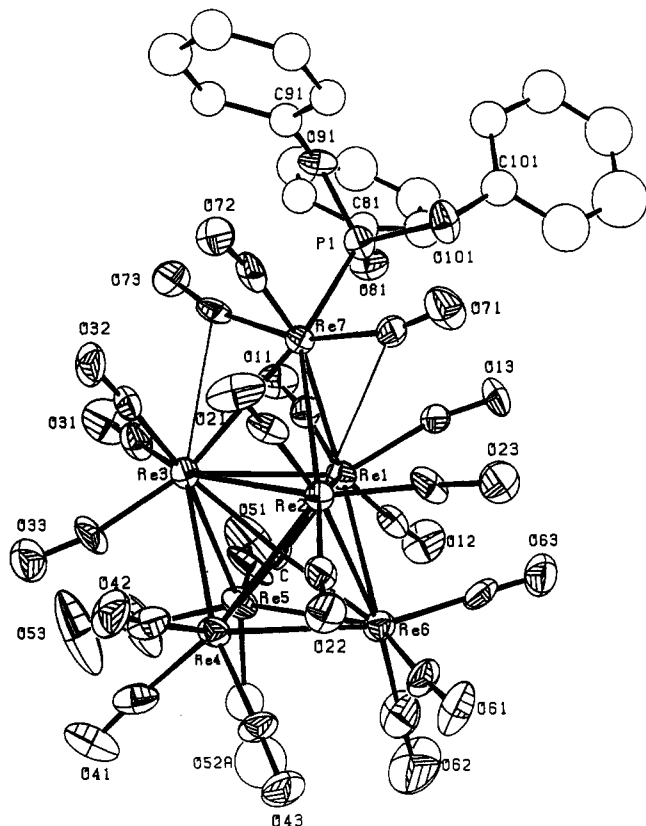
	x/a	y/b	z/c
Re1	0.07536 (5)	0.18156 (5)	0.21024 (3)
Re2	0.24969 (5)	0.26401 (5)	0.26068 (3)
Re3	0.06416 (5)	0.38656 (5)	0.25204 (3)
Re4	0.11080 (6)	0.31986 (5)	0.37848 (4)
Re5	–0.06586 (6)	0.23945 (6)	0.32653 (4)
Re6	0.13259 (6)	0.11115 (5)	0.33269 (4)
Re7	0.19985 (5)	0.31428 (5)	0.13100 (3)
C	0.094 (1)	0.247 (1)	0.2958 (8)
C11	–0.014 (1)	0.220 (1)	0.1525 (9)
O11	–0.082 (1)	0.245 (1)	0.1232 (6)
C12	–0.005 (1)	0.069 (1)	0.2220 (9)
O12	–0.052 (1)	0.0040 (10)	0.2233 (7)
C13	0.176 (2)	0.104 (1)	0.1519 (8)
O13	0.233 (1)	0.0473 (9)	0.1254 (6)
C21	0.330 (1)	0.372 (1)	0.2343 (8)
O21	0.377 (1)	0.436 (1)	0.2228 (7)
C22	0.322 (1)	0.267 (1)	0.3316 (9)
O22	0.378 (1)	0.2701 (9)	0.3681 (6)
C23	0.348 (1)	0.157 (2)	0.2371 (9)
O23	0.409 (1)	0.091 (1)	0.2255 (7)
C31	–0.061 (2)	0.424 (1)	0.2206 (9)
O31	–0.137 (1)	0.448 (1)	0.2005 (8)
C32	0.138 (1)	0.499 (1)	0.2224 (9)
O32	0.177 (1)	0.5662 (9)	0.2078 (7)
C33	0.008 (1)	0.473 (2)	0.3201 (10)
O33	–0.032 (1)	0.536 (1)	0.3525 (7)
C41	–0.002 (2)	0.367 (2)	0.439 (1)
O41	–0.067 (1)	0.394 (1)	0.4777 (8)
C42	0.186 (2)	0.426 (2)	0.3967 (10)
O42	0.234 (1)	0.4879 (9)	0.4044 (7)
C43	0.157 (2)	0.254 (1)	0.4473 (9)
O43	0.180 (1)	0.214 (1)	0.4912 (7)
C51	–0.166 (2)	0.204 (2)	0.279 (1)
O51	–0.231 (1)	0.191 (1)	0.2497 (9)
C52A	–0.130 (2)	0.185 (2)	0.400 (1)
O52A	–0.162 (2)	0.137 (2)	0.443 (1)
C52B	–0.119 (5)	0.135 (3)	0.371 (3)
O52B	–0.165 (4)	0.074 (4)	0.397 (3)
C53	–0.165 (2)	0.337 (2)	0.361 (1)
O53	–0.223 (2)	0.400 (2)	0.376 (1)
C61	0.242 (2)	0.081 (1)	0.3763 (10)
O61	0.315 (1)	0.0587 (10)	0.4009 (8)
C62	0.050 (2)	0.031 (2)	0.389 (1)
O62	0.006 (2)	–0.018 (1)	0.422 (1)
C63	0.176 (2)	–0.001 (1)	0.2847 (10)
O63	0.197 (1)	–0.071 (1)	0.2554 (7)
C71	0.338 (2)	0.241 (1)	0.1222 (9)
O71	0.419 (1)	0.207 (1)	0.1037 (7)
C72	0.280 (2)	0.420 (1)	0.1051 (9)
O72	0.322 (1)	0.4873 (9)	0.0950 (6)
C73	0.082 (1)	0.400 (1)	0.1111 (8)
O73	0.0281 (10)	0.4511 (10)	0.0872 (6)
P1	0.1938 (3)	0.2595 (3)	0.0295 (2)
O81	0.0943 (9)	0.2071 (9)	0.0242 (6)
C82	0.015 (1)	0.1138 (7)	–0.0420 (7)
C83	–0.056 (1)	0.1045 (7)	–0.0831 (7)
C84	–0.113 (1)	0.1859 (7)	–0.1017 (7)
C85	–0.099 (1)	0.2766 (7)	–0.0792 (7)
C86	–0.028 (1)	0.2858 (7)	–0.0381 (7)
C81	0.029 (1)	0.2044 (7)	–0.0195 (7)
O91	0.1891 (8)	0.3371 (8)	–0.0267 (5)
C92	0.3595 (9)	0.3939 (7)	–0.0459 (6)
C93	0.4203 (9)	0.4709 (7)	–0.0575 (6)
C94	0.3744 (9)	0.5643 (7)	–0.0609 (6)
C95	0.2676 (9)	0.5808 (7)	–0.0527 (6)
C96	0.2068 (9)	0.5039 (7)	–0.0411 (6)
C91	0.2527 (9)	0.4104 (7)	–0.0377 (6)
O101	0.2855 (9)	0.1816 (8)	0.0041 (6)
C102	0.300 (1)	0.019 (1)	–0.0278 (6)
C103	0.298 (1)	–0.052 (1)	–0.0725 (6)
C104	0.279 (1)	–0.027 (1)	–0.1329 (6)
C105	0.262 (1)	0.070 (1)	–0.1487 (6)
C106	0.265 (1)	0.142 (1)	–0.1041 (6)
C101	0.283 (1)	0.116 (1)	–0.0436 (6)

^a Relative occupancy 0.67 (2) for disordered carbonyl positions 52A/52B.

- Ciani, G.; D'Alfonso, G.; Freni, M.; Romiti, P.; Sironi, A. *J. Chem. Soc., Chem. Commun.* **1982**, 339.
- Beringhelli, T.; D'Alfonso, G.; Ciani, G.; Sironi, A.; Molinari, H. *J. Chem. Soc., Dalton Trans.* **1988**, 1281.
- Beringhelli, T.; D'Alfonso, G.; Ciani, G.; Sironi, A.; Molinari, H. *J. Chem. Soc., Dalton Trans.* **1990**, 1901.
- Beringhelli, T.; D'Alfonso, G.; Freni, M.; Ciani, G.; Sironi, A. *J. Organomet. Chem.* **1985**, 295, C7.
- Henly, T. J.; Shapley, J. R.; Rheingold, A. L. *J. Organomet. Chem.* **1986**, 310, 55.
- Henly, T. J.; Shapley, J. R.; Rheingold, A. L.; Geib, S. J. *Organometallics* **1988**, 7, 441.
- Henly, T. J.; Wilson, S. R.; Shapley, J. R. *Inorg. Chem.* **1988**, 27, 2551.
- Ma, L.; Wilson, S. R.; Shapley, J. R. *Inorg. Chem.* **1990**, 29, 5133.
- Evans, D. G.; Mingos, D. M. P. *Organometallics* **1983**, 2, 435.

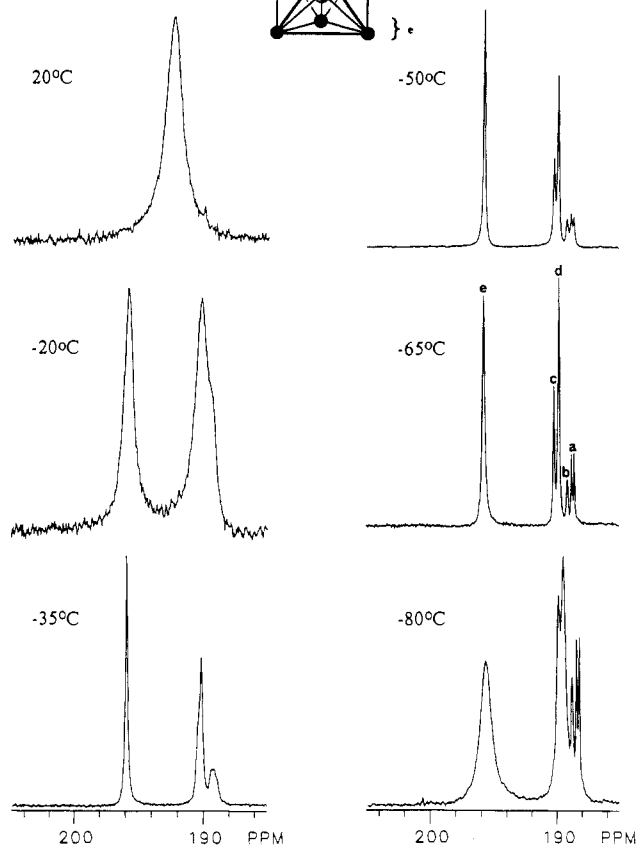
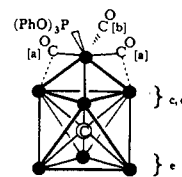
Table III. Selected Bond Lengths (Å) and Bond Angles (deg) for $[\text{PPN}][\text{Re}_7\text{C}(\text{CO})_{21}(\text{P}(\text{O}Ph)_3)]$

Re1–Re2	3.003 (1)	Re1–Re3	2.990 (1)	Re2–Re3	2.892 (1)
Re2–Re4	2.970 (1)	Re3–Re4	2.995 (1)	Re1–Re5	2.966 (1)
Re3–Re5	3.077 (1)	Re4–Re5	3.032 (1)	Re1–Re6	2.977 (1)
Re2–Re6	3.023 (1)	Re4–Re6	3.058 (1)	Re5–Re6	3.062 (1)
Re1–Re7	2.946 (1)	Re2–Re7	3.018 (1)	Re3–Re7	3.062 (1)
Re7–P	2.334 (5)	Re7–C71	2.00 (2)	Re7–C72	1.92 (2)
Re7–C73	1.97 (2)	Re–C (av)	2.12 (3)	Re–CO (av)	1.92 (4)
Re1–Re7–Re2	60.44 (2)	Re1–Re7–Re3	59.66 (2)	Re2–Re7–Re3	56.80 (2)
Re1–Re7–P	102.8 (1)	Re2–Re7–P	146.7 (1)	Re3–Re7–P	142.8 (1)
C71–Re7–P	85.3 (5)	C72–Re7–P	95.6 (6)	C73–Re7–P	81.1 (5)
C71–Re7–C73	160.7 (7)	Re1–Re2–Re3	60.93 (2)	Re1–Re3–Re2	61.36 (2)
Re7–C71–O71	165 (2)	Re7–C72–O72	176 (2)	Re7–C73–O73	165 (2)

**Figure 1.** ORTEP diagram of the cluster anion in $[\text{PPN}][\text{Re}_7\text{C}(\text{CO})_{21}(\text{P}(\text{O}Ph)_3)]$ showing the atomic labeling scheme (35% probability ellipsoids).

fragment, particularly when the carbonyl ligands can form large secondary bonding interactions with adjacent metal centers. Two symmetric conformations are possible: one in which the plane containing the pseudo-trans semibringing carbonyl ligands bisects a metal–metal bond and one in which this plane is parallel to a metal–metal bond. There is little calculated difference in energy for the two conformations. The capping ML_4 moiety in $[\text{Re}_7\text{C}(\text{CO})_{21}(\text{P}(\text{O}Ph)_3)]^-$ adopts the latter orientation, which provides the opportunity for two equivalent semibringing interactions, and displays one large interligand angle ($\angle(\text{C}71-\text{Re}7-\text{C}73) = 160.7(7)^\circ$) and one small one ($\angle(\text{P}1-\text{Re}7-\text{C}72) = 95.6(6)^\circ$). Essentially the same geometry is shown in $\text{H}_2\text{Ru}_4(\text{CO})_{13}$ ²¹ and $\text{H}_2\text{FeRu}_3(\text{CO})_{13}$.²² Interestingly, in $[\text{HRe}_5\text{C}(\text{CO})_{16}]^{2-}$,²³ which also contains four carbonyls bonded to one metal center, only one semibringing carbonyl is utilized to balance the electronic distribution.

Solution Stereodynamics of $[\text{Re}_7\text{C}(\text{CO})_{21}(\text{P}(\text{O}Ph)_3)]^-$ and $[\text{Re}_7\text{C}(\text{CO})_{22}]^-$. Variable-temperature ^{13}C NMR spectra (car-

**Figure 2.** Variable-temperature ^{13}C NMR spectra (90 MHz) of $[\text{PPN}][\text{Re}_7\text{C}(\text{CO})_{21}(\text{P}(\text{O}Ph)_3)]$ in dichloromethane.

bonyl region) of $[\text{Re}_7\text{C}(\text{CO})_{21}(\text{P}(\text{O}Ph)_3)]^-$ are shown in Figure 2. At room temperature, $[\text{Re}_7\text{C}(\text{CO})_{21}(\text{P}(\text{O}Ph)_3)]^-$ displays only one broad signal at δ 192.7. Below ca. -50°C , the resonance is split into a pattern of signals that persists to the lowest temperature reached (-80°C). This pattern (δ 188.5 (d) ($J_{\text{P-C}} = 21$ Hz), 2C), 189.0 (1C), 189.7 (6C), 190.1 (3C), 195.6 (9C) at -65°C) is readily assigned in terms of the solid-state structure. The doublet is assigned to the two equivalent semibringing carbonyls (a) cis to the phosphite ligand on the capping rhenium moiety. The adjacent broad singlet is the single carbonyl ligand (b) "trans" to the phosphite ligand. The two signals with a 3:6 intensity ratio are assigned to the carbonyls attached to the three rhenium atoms in the capped face (c and d), presumably made distinct by the semibringing interactions. The remaining signal is due to the nine carbonyls (e) attached to the basal plane of three rhenium atoms; observable broadening of this signal at -80°C implies

(21) Yawney, D. B.; Doedens, R. *J. Inorg. Chem.* **1972**, *11*, 838.(22) Gilmore, C. J.; Woodward, P. *J. Chem. Soc. A* **1971**, 3453.(23) Henly, T. J.; Wilson, S. R.; Shapley, J. R. *Organometallics* **1987**, *6*, 2618.

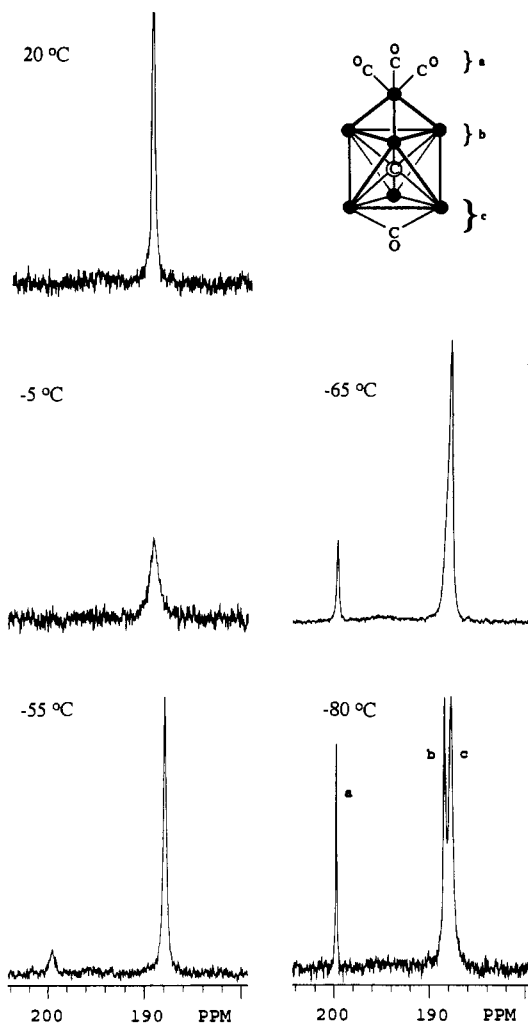


Figure 3. Variable-temperature ^{13}C NMR spectra (125 MHz) of [PPN]- $[\text{Re}_7\text{C}(\text{CO})_{22}]^-$ in dichloromethane.

that site exchange is approaching the intermediate exchange rate at this temperature.

Variable temperature ^{13}C NMR spectra of $[\text{Re}_7\text{C}(\text{CO})_{22}]^-$ are shown in Figure 3. The single peak at δ 190.0 observed at room temperature broadens at lower temperatures and splits into two signals at δ 199.9 (3C) and δ 188.0 (19C). The latter resonance splits further into two signals (ca. 9:10 ratio) at -80°C . The lowest field signal at δ 199.9 is assigned to three carbonyls attached to a capping rhenium center, on the basis of comparisons with the pattern of signals from other heptarhenium clusters.^{10,14,16-19,24,25} The higher field signals are assigned to carbonyls located on the two triangles of rhenium atoms. Below -80°C (not shown), the more upfield, larger one of these signals broadens and begins to collapse. This suggests that it is due to the carbonyls attached to the basal (noncapped) triangle of rheniums, since internuclear scrambling involving a bridging carbonyl should be less facile than localized 3-fold rotation.

These ^{13}C NMR data imply that both $[\text{Re}_7\text{C}(\text{CO})_{22}]^-$ and $[\text{Re}_7\text{C}(\text{CO})_{21}(\text{P}(\text{O}Ph)_3)]^-$ retain their separate and distinct solid-state structures in solution. Nevertheless, each compound also shows complete and rapid scrambling of its carbonyl ligands at room temperature. This feature contrasts sharply with the situation for $[\text{Re}_7\text{C}(\text{CO})_{21}]^{3-}$, which exhibits significantly slower carbonyl scrambling that does not extend to the $\text{Re}(\text{CO})_3$ cap.²⁴

Charge Separation in $[\text{Re}_7\text{C}(\text{CO})_{21}(\text{P}(\text{O}Ph)_3)]^-$ and Conversion to $[\text{Re}_6\text{C}(\text{CO})_{19}]^{2-}$. The carbonyl ^{13}C NMR spectrum of

$[\text{Re}_7\text{C}(\text{CO})_{21}(\text{P}(\text{O}Ph)_3)]^-$ is unique as well in terms of the chemical shifts of the different types of carbonyls. For all other heptarhenium clusters, the signals for the carbonyls attached to the capping rhenium center, in these cases $\text{Re}(\text{CO})_3$, appear at lower field by ca. 10 ppm than the signals for the carbonyls attached to the rhenium atoms of the octahedral core.^{12,14,16-19,24,25} For $[\text{Re}_7\text{C}(\text{CO})_{21}(\text{P}(\text{O}Ph)_3)]^-$ the signals for the carbonyls attached to the rhenium cap (a,b in Figure 2) are actually at higher field than those for the carbonyls bonded to the core rhenium atoms (c-e in Figure 2). Furthermore, the latter signals as a group are shifted downfield ca. 5 ppm relative to the analogous set in $[\text{Re}_7\text{C}(\text{CO})_{22}]^-$. Therefore, the pattern of ^{13}C NMR chemical shifts for $[\text{Re}_7\text{C}(\text{CO})_{21}(\text{P}(\text{O}Ph)_3)]^-$ suggests a picture of charge separation, with a relatively positive $\{\text{Re}(\text{CO})_3\text{L}\}(1+)$ cap interacting with a relatively negative $[\text{Re}_6(\mu_6\text{-C})(\text{CO})_{18}](2-)$ core. This feature presumably contributes to the difference in structure with respect to $[\text{Re}_7\text{C}(\text{CO})_{22}]^-$ in that the better donor ligand is in position to stabilize the positively charged center.

Charge separation, such as shown in $[\text{Re}_7\text{C}(\text{CO})_{21}(\text{P}(\text{O}Ph)_3)]^-$, is undoubtedly a necessary stage in decapping reactions involving polar species, but the intermediates are seldom isolated.²⁶ Similar oxidation of one cluster vertex was observed in $[\text{Fe}_5\text{C}(\text{CO})_{12}\text{Br}_2]^{2-}$, which was identified by Bradley²⁷ as a probable intermediate in the transformation of $\text{Fe}_5\text{C}(\text{CO})_{15}$ into $[\text{Fe}_4\text{C}(\text{CO})_{12}]^{2-}$. Evidence for multiple attack by nucleophiles at a single vertex of $\text{Os}_6(\text{CO})_{18}$, pertaining especially to the conversion to $[\text{Os}_5(\text{CO})_{15}]^{2-}$, has been provided in extensive studies by Johnson and Lewis.^{28,29} The overall process of decomposing the $\{\text{Re}_7\text{C}\}$ framework into $[\text{Re}_6\text{C}(\text{CO})_{19}]^{2-}$ and a rhenium(I) moiety has been effected by treatment of $[\text{Re}_7\text{C}(\text{CO})_{21}]^{3-}$ with $\text{Cp}_2\text{Fe}^+/\text{PPh}_3$ in acetone,⁹ with I_2 in acetonitrile,⁸ and, as shown herein, with $\text{Cp}_2\text{Fe}^+/\text{P}(\text{O}Ph)_3$ in acetonitrile, producing the primary coproducts $[\text{Re}(\text{CO})_4(\text{PPh}_3)_2]^+$, $\text{Re}(\text{CO})_3(\text{NCCH}_3)_2\text{I}$, and $[\text{Re}(\text{CO})_3(\text{P}(\text{O}Ph)_3)_2(\text{NCCH}_3)]^+$, respectively. Furthermore, direct treatment with acetonitrile fragments $[\text{Re}_7\text{C}(\text{CO})_{22}]^-$ into $[\text{Re}_6\text{C}(\text{CO})_{19}]^{2-}$ and $[\text{Re}(\text{CO})_3(\text{NCCH}_3)_3]^+$,^{8,9} similar treatment of $[\text{H}_2\text{Re}_7\text{C}(\text{CO})_{21}]^-$ was shown to provide $[\text{H}_2\text{Re}_6\text{C}(\text{CO})_{18}]^{2-}$.¹⁴ The ability of acetonitrile to "open up" cluster vertexes has been illustrated in the case of $\text{Ru}_5\text{C}(\text{CO})_{15}$ with the structural characterization of an adduct.²⁸ Analogous reactions of $\text{Os}_5(\text{CO})_{16}$ and $\text{Os}_6(\text{CO})_{18}$ with carbon monoxide have been shown to convert $\text{Os}(\text{CO})_3$ caps into $\text{Os}(\text{CO})_4$ flaps as an intermediate stage prior to complete cleavage of $\text{Os}(\text{CO})_5$.³⁰ However, these decapping reactions do not involve polar species, and improved understanding and control of polar fragmentation reactions should benefit from further study of charge-separated cluster compounds.

Acknowledgment. This research was supported by National Science Foundation Grant DMR 89-20538 to the Materials Research Laboratory at the University of Illinois.

Supplementary Material Available: Tables of positional and thermal parameters and a complete list of bond distances and angles (20 pages). Ordering information is given on any current masthead page.

(24) Simerly, S. W.; Shapley, J. R. *Inorg. Chem.* 1990, 29, 3634.

(25) Folkers, J. P.; Hayward, C.-M.; Shapley, J. R. *Inorg. Chem.* 1988, 27, 3685.

(26) Vargas, M. D.; Nicholls, J. N. *Adv. Inorg. Chem. Radiochem.* 1986, 30, 123.

(27) Bradley, J. S.; Hill, E. W.; Ansell, G. B.; Modrick, M. A. *Organometallics* 1982, 1, 1634.

(28) Johnson, B. F. G.; Lewis, J.; McPartlin, M.; Pearsall, M.-A.; Sironi, A. *J. Chem. Soc., Chem. Commun.* 1984, 1089.

(29) Johnson, B. F. G.; Lewis, J.; Nicholls, J. N.; Puga, J.; Raithby, P. R.; Rosales, M. J.; McPartlin, M.; Clegg, W. *J. Chem. Soc., Dalton Trans.* 1983, 277.

(30) Farrar, D. H.; Johnson, B. F. G.; Lewis, J.; Raithby, P. R.; Rosales, M. J. *J. Chem. Soc., Dalton Trans.* 1982, 2051.